**SUPPLEMENTARY INFORMATION**

# *Trans-Cis* Isomerization of Lipophilic Dyes Probing Membrane Microviscosity in Biological Membranes and in Live Cells.

Volodymyr Chmyrov, Thiemo Spielmann, Heike Hevekerl, Jerker Widengren[1]
Experimental Biomolecular Physics, Department of Applied Physics,
Royal Institute of Technology, Stockholm, Sweden.

Table of contents



[1] Corresponding author: Jerker Widengren,
Email: jerker@biomolphysics.kth.se

## THEORY

### Electronic state model.

The photodynamic model used for the dye Merocyanine 540 (MC540) is shown in Figure S1. At equilibrium, with no excitation, MC540 adopts an all-*trans* conformation. Upon excitation, one of the double bounds in the polymethine chain of the dye can undergo a $\pi$-twist around the bond axis and the molecule switches into a non-fluorescent *cis* isomer. Likewise, when in a *cis* state, excitation-driven back-isomerization can take the MC540 molecule back to an all-*trans* state. These transitions, and the states involved are defined in Figure 1B, where also a more detailed description of the model is given.

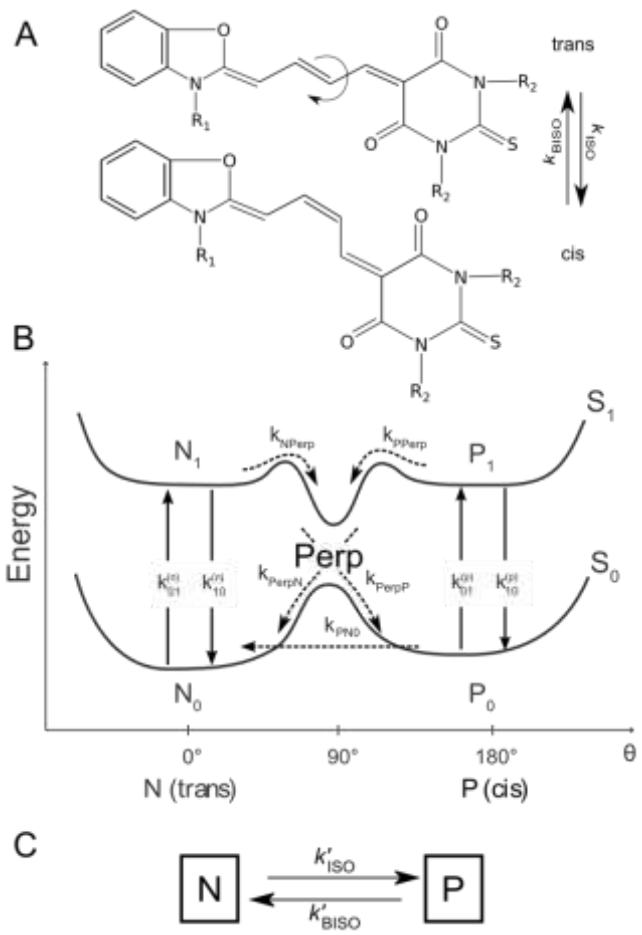


Figure S1: **(A)**: Chemical structure and conformations of the *trans* and *cis* isomers of Merocyanine 540. **(B)**: Generally used model for *trans-cis* isomerization of cyanine dyes, where the horizontal direction corresponds to the torsion angle around a double bond of the polymethine chain of MC540, and the vertical direction corresponds to Energy. $N_0$ and $N_1$ denote the ground singlet and the first excited singlet state of the all-*trans* form. $k_{01}^{(n)} = \sigma_N I_{exc}$ and $k_{01}^{(n)}$ are the rates of excitation from $N_0$ to $N_1$, and deactivation from $N_1$ to $N_0$. $P_0$ and $P_1$, and $k_{01}^{(p)} = \sigma_p I_{exc}$ and $k_{01}^{(p)}$ are the corresponding states and rates of the mono-*cis* form. $Perp$ is the intermediary twisted excited state at half the rotation angle. It is formed from $N_1$ or $P_1$ at rates $k_{NPerp}$ and $k_{PPerp}$, respectively, and deactivated in the picosecond to nanosecond range to either $N_0$ or $P_0$. $P_0$ can thermally relax to the ground state of the all-*trans* form, $N_0$, with a rate denoted by $k_{PN0}$. This transition typically takes place in the millisecond time range. **(C)**: Simplified photophysical model for cyanine dyes, with for our FCS and TRAST measurements relevant simplifications, supported by observations made for other cyanine dyes[1, 2]. Transitions to and from the partially twisted intermediate state, $Perp$, as well as transitions between the singlet states within the *trans* and *cis* forms are disregarded since they take place on a time scale much faster than the switching between the *trans* and *cis* isomers. The $Perp$ state is typically deactivated in the picosecond to

nanosecond time scale to either $N_0$ or $P_0$, and the deactivation times of $N_1$ and $P_1$ are in the nanosecond time scale. These transitions will therefore not be resolved on the time scale of the FCS and TRAST measurements. Since most *cis*-isomers of thiacarbocyanine dyes are believed not to fluoresce at room temperature, and upon excitation to mainly be deactivated through internal conversion the fluorescence brightness of the *cis* photo-isomer can be neglected. Triplet state formation from either $N_1$ or $P_1$ is also in general very low for thiacarbocyanine dyes, and can therefore be disregarded in the model, and for the measurement conditions used in this study.

Based on time-averaging of the fast transitions between the states of Figure S1B and disregarding any triplet state formation in the dyes, the kinetic schedule of Figure S1B can be simplified to the two-state model of Figure S1C, containing a fluorescent *trans* form N ($N_0$ and $N_1$) and a non-fluorescent *cis* form P ($P_0$ and $P_1$). The effective transition rate constants from N and P will be the same as those from the excited state levels of N and P, except for a scaling factor corresponding to the fractions of dyes in the N and P forms that are in their excited singlet states:

$$k'_{ISO} = k_{ISO}\frac{k_{01}^{(N)}}{k_{01}^{(N)}+k_{10}^{(N)}} = k_{ISO}\frac{\sigma_N I_{exc}}{\sigma_N I_{exc}+k_{10}^{(N)}} \qquad \text{(S1)}$$

$$k'_{BISO} = k_{BISO}\frac{k_{01}^{(P)}}{k_{01}^{(P)}+k_{10}^{(P)}} + k_{PN0}$$

$$= k_{BISO}\frac{\sigma_P I_{exc}}{\sigma_P I_{exc}+k_{10}^{(P)}} + k_{PN0} \qquad \text{(S2)}$$

$$= \left\{k_{10}^{(P)} \gg \sigma_P I_{exc}\right\} = \sigma_{BISO} I_{exc} + k_{PN0}$$

where $I_{exc}$ is the excitation intensity, $\sigma_N$ and $\sigma_P$ are the excitation cross sections of the $N_0$ and $P_0$ states, and $\sigma_{BISO} = \frac{k_{BISO}}{k_{10}^{(p)}}\sigma_P$ denotes the effective cross section for back-isomerization of the *cis* state.

**Fluorescence Correlation Spectroscopy (FCS).**

Based on a confocal, epi-illuminated instrument, the detected fluorescence rate in the FCS measurements is given by:

$$F(t) = \int CEF(\bar{r})c(\bar{r},t)k_{10}^{(N)}q\Phi_f N_1(\bar{r},t)dV \qquad \text{(S3)}$$

Here, $CEF(\bar{r})$ is the collection efficiency function of the confocal microscope setup, $c(\bar{r},t)$ denotes the concentration of fluorophores. $q$ the quantum efficiency of the detectors and the attenuation of the fluorescence in the passage from the sample volume to the detector areas, $\Phi_f$ the fluorescence quantum yield of the fluorophore, and $N_1(\bar{r},t)$ the fraction of the fluorophores that are in their excited singlet *trans* states. The fluorescence fluctuations are caused by changes in $N_1(\bar{r},t)$ and by changes in $c(\bar{r},t)$, caused by translational motion of the fluorophores into and out of the detection volume. If fluorescence fluctuations arise from translational diffusion, assuming a 3-dimensional Gaussian distribution of the detected fluorescence, and from fluorescence blinking originating from transitions between a fluorescent *trans* isomer, $N$, and a non-fluorescent *cis* isomer, $P$, as modeled in Figure S1C, the time dependent part of the correlation function takes the form[1, 2]:

$$G(\tau) - 1 = \frac{1}{N_m}\left[1+\frac{\tau}{\tau_D}\right]^{-1} \times \left[1+\left(\frac{\omega_0}{\omega_z}\right)^2\frac{\tau}{\tau_D}\right]^{-\frac{1}{2}}\left[1+\frac{P_{eq}}{1-P_{eq}}exp(-\tau/\tau_{ISO})\right] \qquad \text{(S4)}$$

Here $\omega_0$ and $\omega_Z$ are the distances from the center of the laser beam focus in the radial and axial direction respectively at which the collected fluorescence intensity has dropped by a factor of $1/e^2$ compared to its peak value. $N_m$ is the mean number of fluorescent molecules within the detection volume. $\tau_D$ is the characteristic diffusion time of the fluorescent molecules, given by the diffusion coefficient $D$ as $\tau_D = \omega_0^2/4D$. $P_{eq}$ is the time and space averaged fraction of fluorophores within the detection volume being in a non-fluorescent *cis* photoisomer form, and $\tau_{ISO}$ is the relaxation time related to the

*trans-cis* isomerization process. Approximating the excitation irradiance distribution within the detection volume to be uniform[1-3], $P_{eq}$ and $\tau_{ISO}$ of Equation 4 can be written as:

$$P_{eq} = \frac{k'_{ISO}}{k'_{ISO}+k'_{BISO}} \quad \text{(S5)}$$

$$\tau_{ISO} = (k'_{ISO} + k'_{BISO})^{-1} \quad \text{(S6)}$$

**Transient state (TRAST) imaging**

For a MC540 molecule subject to a train of rectangular excitation laser pulses of height $I_{exc}$ and duration $t_p$, the time dependence of the fluorophore to be in a *trans* state, $N(t)$, can be described by the model of Figure S1C. Following the model of Figure S1C, $N(t)$ is obtained via a system of linear differential equations which in matrix form can be written as:

$$\frac{d}{dt}\vec{S}(t) = \mathbf{M}\vec{S}(t) \quad \text{(S7)}$$

$$\vec{S}(t) = \begin{pmatrix} N(t) \\ P(t) \end{pmatrix} \quad \mathbf{M} = \begin{pmatrix} -k'_{ISO} & k'_{BISO} \\ k'_{ISO} & -k'_{BISO} \end{pmatrix} \quad \text{(S8)}$$

Here, $\vec{S}$ is the population vector of the *trans*, $N$, and *cis*, $P$, states and $\mathbf{M}$ is a coupling matrix.

The eigenvalues of $\mathbf{M}$ are given by:

$$\begin{cases} \lambda_1 = 0 \\ \lambda_2 = -k'_{ISO} - k'_{BISO} \end{cases} \quad \text{(S9)}$$

and the corresponding pair of orthogonal eigenvectors by:

$$\vec{v}_1 = \begin{pmatrix} k'_{BISO} \\ k'_{ISO} \end{pmatrix}, \quad \vec{v}_2 = \begin{pmatrix} -1 \\ 1 \end{pmatrix} \quad \text{(S10)}$$

Ideally in a TRAST experiment, applying a train of rectangular excitation pulses with a low duty cycle, the non-fluorescent transient state(s) should within the time between the pulses ($T_p - t_p$, with $T_p$ denoting the period time) relax back to the ground state of the fluorescent form of the dye. However, the isomerization to and from P are mainly excitation-driven (Figure S1B). In the absence of excitation there is only a slow thermal deactivation rate, $k_{PN0}$, of P, typically in the range of 0,1-1 $ms^{-1}$. The *cis* state does therefore not necessarily relax back completely to the ground *trans* state during the off-periods, i.e. in between the excitation pulses of the pulse trains used in the TRAST experiments.

For a correct representation of the fluorescence response to a rectangular pulse train of arbitrary duty cycle, the solution to Equation S1 that can be written as:

$$\vec{S}(t) = \sum c_i \vec{v_i} \exp(\lambda_i t) = \mathbf{Q}\exp(\mathbf{\Lambda} t)\vec{C} \quad \text{(S11)}$$

which could then be rewritten in the form of a propagator:

$$\vec{S}(t) = \mathbf{Q}\exp(\mathbf{\Lambda} t)\mathbf{Q^{-1}}\vec{S}(t_0) = \mathbf{U}(t, t_0)\vec{S}(t_0) \quad \text{(S12)}$$

Where $\vec{v_i}$ and $\lambda_i$ are eigenvectors and eigenvalues respectively. $c_i$ represents a set of constants, obtained from the initial conditions to Equation S1. $\mathbf{\Lambda_{ii}} = \lambda_i$ is the diagonal eigenvalue matrix, $\mathbf{Q}$ is the eigenvector matrix having as its i-th column the eigenvector $\vec{v_i}$. $\vec{C}$ is a vector containing the constants $c_i$. The matrix $\mathbf{U}(t, t_0)$ describes how the system evolves over time from an initial state $\vec{S}(t)$.

$$\mathbf{Q} = \begin{pmatrix} k'_{BISO} & -1 \\ k'_{ISO} & 1 \end{pmatrix} \qquad \mathbf{Q^{-1}} = \frac{1}{k'_{ISO}+k'_{BISO}}\begin{pmatrix} 1 & -1 \\ -k'_{ISO} & k'_{BISO} \end{pmatrix} \quad \text{(S13)}$$

Taking into account that $\forall t$, $N(t) + P(t) = 1$, arbitrary initial conditions $\vec{S}(t_0)$ can be written as:

$$\vec{S}(t_0) = \begin{pmatrix} 1-P(t_0) \\ P(t_0) \end{pmatrix} \quad \text{(S14)}$$

The evolution of the solution of the initial system (Equation S7) can then be calculated as a function of an arbitrary initial population of the cis-state $P(t_0)$:

$$\binom{N(t)}{P(t)} = \begin{cases} \frac{k'_{BISO}}{k'_{BISO}+k'_{ISO}} + \left(\frac{k'_{BISO}}{k'_{BISO}+k'_{ISO}} - P(t_0)\right)\exp(\lambda_2 t) \\ \frac{k'_{ISO}}{k'_{BISO}+k'_{ISO}} - \left(\frac{k'_{ISO}}{k'_{BISO}+k'_{ISO}} - P(t_0)\right)\exp(\lambda_2 t) \end{cases} \quad \text{(S15)}$$

By use of Equation S15, and for a fluorophore subject to a rectangular excitation pulse train (with $N_P$ number of pulses, pulse period $T_P$, and duration of pulses $t_p$), and resetting the time $t$ in Equation 9 to zero after each period of the excitation pulse train, the average population of $N = N_0 + N_1$within the excitation pulses can be obtained from the last sum over the integrals part of Equation S15 as:

$$\langle N\rangle_{t_{exp}}(t_p) = \frac{1}{N_p t_p}\sum_{i=0}^{N_p-1}\int_{iT_p}^{iT_p+t_p} N(t)dt =$$

$$= \int_0^{t_p}\frac{1}{N_p t_p}\sum_{j=1}^{N_p}\left[\frac{k'_{BISO}}{-\lambda_2} + \left(\frac{k'_{ISO}}{-\lambda_2} - P_j(0)\right)\exp(\lambda_2 t)\right]dt \quad \text{(S16),}$$

where $P_j(0)$ is the *cis* state population at the onset of the j'th pulse. Since all rates and eigenvalues are constant over $t \in [0, t_p]$ integration yields:

$$\langle N\rangle_{t_{exp}}(t_p) = \frac{1}{t_p}\left[\left(\frac{k'_{BISO}}{-\lambda_2^2} + \frac{1}{\lambda_2}\langle P_{init}\rangle\right)\left(1 - \exp(\lambda_2 y)\right) + \frac{k'_{BISO}}{\lambda_2}t_p\right] \quad \text{(S17)}$$

Here, the time averaged population of the *trans* state for a pulse train of pulse width $t_p$, denoted $\langle N\rangle_{t_{exp}}(t_p)$, involves the average initial occupancy of the *cis* state at the onset of all the pulses within the pulse train: $\langle P_{init}\rangle = \frac{1}{N_p}\sum_{j=1}^{N_p}\left(P_j(0)\right)$.

In order to calculate $\langle P_{init}\rangle$ a propagator was defined for the time during which the pulse is on $\mathbf{U}^{on}(t_p, 0)$ and one for which the excitation is off $\mathbf{U}^{off}(T_p, t_p)$. For $\mathbf{U}^{off}(T_p, t_p)$, $k'_{ISO} = 0$ and $k'_{BISO} = k_{PN0}$ since by definition $I_{exc}$ is equal to zero during the off-times. The evolution of the populations at time $t = T_p$, after one full pulse period starting at $t_0 = 0$ is then given by:

$$\vec{S}(T_p) = \mathbf{U}^{off}(T_p, t_p)\mathbf{U}^{on}(t_p, 0)\vec{S}(t_0) \quad \text{(S18)}$$

Similarly, the population status of N and P at $t = t_{exp} = N_p T_p$, after a full pulse train consisting of NP pulses, is found by applying the $N_p$times the propagator.

$$\vec{S}(N_p T_p) = \left(\mathbf{U}^{off}(T_p, t_p)\mathbf{U}^{on}(t_p, 0)\right)^{N_p}\vec{S}(t_0) \quad \text{(S19)}$$

Finally, the propagators can be used in order to calculate $\langle P_{init}\rangle$, as well as the average population of N and P at the onset of an excitation pulse within the pulse train:

$$\binom{\langle N_{init}\rangle}{\langle P_{init}\rangle} = \frac{1}{N_p}\sum_{j=0}^{N_p-1}\binom{\langle N_j(0)\rangle}{\langle P_j(0)\rangle} = \frac{1}{N_p}\sum_{j=0}^{N_p-1}\left[\mathbf{U}^{off}(T_p, t_p)\mathbf{U}^{on}(t_p, 0)\right]^j\vec{S}(t_0)$$

(S20)

## MATERIALS AND METHODS

### Sample preparation.

A 2 mM stock solution of Merocyanine 540 (MC540, Sigma-Aldrich) was prepared in ethanol. DOPC, DOPG and cholesterol (Avanti Polar Lipids) were obtained dissolved in Chloroform (10mg/mL) or as a powder. DOPC and DOPG liposomes were prepared as previously described[4], in a 0.2 mM, pH 7.4 KCl solution, and cholesterol in varying percentages

was included when stated. For the liposome formation, a mini-extruder (Avanti) with membrane filters containing 30, 50, 100 and 200 nm diameter pores was used. For the FCS measurements, the fluorophore-to-lipid ratios were kept quite low (1:1.000.000) for all vesicles sizes to ensure that each liposome had no more than one fluorophore. For the spectrofluorometer measurements the fluorophore-to-lipid ratio was higher (1:30.000). For confocal TRAST measurements, where isomerization kinetics is independent on labeling efficiency, the fluorophore-to-lipid ratio were set relatively high (1:1.000).

For the live cell measurements MCF7 cells were grown adherent in an eight well plate for three to four days. Then cells were washed once with PBS buffer and 300 µL of 5 µM MC540 dissolved in serum free PBS was added to the wells. Cells were incubated for 20 minutes at 37°C, and were then washed three times with a growth medium (containing FBS), with 5 min incubation in between each washing step.

In order to estimate the dimension of the wide field beam, cover slides were labeled with ATTO-Thio 12 (Atto-tec, Siegen, Germany) using Bovine serum albumin (BSA) as a linker. A droplet of BSA solution was deposited on the cover glass slides and incubated for 20 minutes at room temperature. After three washing steps with deionized water, a droplet of PBS solution containing 10 µM of Atto-Thio 12 was applied to the slides. In this step the dye bound to the protein by amine binding. After incubating for at least 10 minutes, the sample was washed 3 times with PBS and kept in this medium until experiment.

**FCS setup.**

The major features of the setup used has previously been described.[5-7] Briefly, for excitation the 568nm line of a krypton-argon laser (Melles Griot 643-RYB-A02, with excitation filter Z568/10, Chroma Technology Corp.) was reflected by a dichroic beam splitter (FF576/661-Di01-18-D, Semrock Inc.) and then focused on the sample by a water-immersion objective (Zeiss, 63x/1.2 Plan-Neofluar, 160 mm tube length, cover glass corrected). In ethanol solutions the laser beam was focused down to radius ($1/e^2$) of 0.35µm, while in the vesicle solution the focal beam radius was 0,7µm. Fluorescence was collected by the same objective, passed through a 50 µm pinhole in the image plane, and focused onto two avalanche photodiodes (APDs) (SPCM-AQR-14, Perkin-Elmer Optoelectronics) in a beam splitting arrangement. Two APDs were used in order to eliminate all influence of the inherent noise, and afterpulsing effects of the detectors. To discriminate background from Raman and Rayleigh scattered laser light, a band-pass filter (HQ640/115M, Chroma Technology Corp.) was inserted in front of each APD. The signal from the two APDs was analyzed by a PC-based correlator (ALV-5000, ALV Gmbh). The laser power was controlled by a laser power controller (BEOC LPC) and measured before the objective by a laser power meter (PM-100, Thor Labs), subsequently corrected for the transmission through the objective.

**TRAST setup.**

The setup used for the TRAST experiments is based on a previously described instrument, with some modifications.[8] The beam of a CW diode-pumped solid state laser (561 nm, 15 mW to 75 mW, Cobolt Jive, Cobolt AB) was focused by a lens (focal distance of 80 mm) into the aperture of an acousto-optic modulator (AOM) (MQ 180-AO, 25-VIS, AA OptoElectronic). After passing the AOM, the beam was collimated by a second lens (focal distance of 300 mm), and then directed either to the back port of a microscope stand (Zeiss 135 TV) or to a home built confocal microscope. For the live-cell measurements at the microscope stand (Zeiss 135 TV), a collimated wide-field beam was generated using a 40× 0.75 Ph2 objective from Zeiss. The microscope stand was equipped with a dichroic mirror (Di01-R561, Semrock) and a fluorescence filter (HQ 610/75, AHF), as well as with an incubation system (Chamlide IC, Live Cell Instrument, Seoul,

Korea) for maintaining constant sample temperatures (variable from room temperature 23 °C to 45 °C). An automatic three gas mixing system (FC-7, LCI) was used to set the partial pressures of $O_2$, $CO_2$ and $N_2$ gas in the incubator. During cell experiments, $O_2$ was kept constant at about 7%, and $CO_2$ at 5% in order to keep the pH of the culturing medium constant.

An electron multiplying CCD camera (658×498 pixels, sized 10 × 10 $\mu m^2$, photon quantum yield of 50%, Luca, Andor Technology), mounted on the camera mount of the microscope stand, was used for imaging the fluorescence emitted from the sample.

For liposome measurements in a confocal arrangement the laser beam was after passage through the AOM directed to another dichroic mirror (Di01-R561, Semrock) and focused on sample by a water immersion objective (Plan-NEOFLUAR 40x/1.2 Zeiss).The fluorescence was collected by the same objective, passed through a fluorescence filter (HQ 610/75, AHF) and directed to the CCD camera where each pixel was considered as a pinhole.

Custom software was used for controlling signal detection and further signal processing. The camera was controlled in Matlab via USB using a driver based on the MCD Software Development Kit from Andor Technology, and the laser via serial port commands. The modulation scheme of the AOM was set via a PCI 6602 card (National Instruments) connected to the AOM controller (AA Opto Electronic).

**Spectrofluorometer measurements.**

Excitation and emission spectra of MC540 in aqueous solution and of MC540-labeled DOPC/Cholesterol liposome solutions were measured by a spectrofluorometer (Fluoromax, Horiba Jobin Yvon). Excitation spectra within 500 to 600 nm were recorded at 640 nm emission, and emission spectra (540 to 650 nm) were recorded at 520 nm excitation.

## REFERENCES


(1) Widengren, J.; Schwille, P. Journal of Physical Chemistry A 2000, 104, (27), 6416-6428.

(2) Widengren, J.; Seidel, C. A. M. Physical Chemistry Chemical Physics 2000, 2, (15), 3435-3441.

(3)Sandén, T.; Persson, G.; Thyberg, P.; Blom, H.; Widengren, J. Analytical Chemistry 2007, 79, (9), 3330-3341.

(4) Sandén, T.; Salomonsson, L.; Brzezinski, P.; Widengren, J. Proceedings of the National Academy of Sciences of the United States of America 2010, 107, (9), 4129-4134.

(5) Strömqvist, J.; Chmyrov, A.; Johansson, S.; Andersson, A.; Mäler, L.; Widengren, J. Biophysical Journal 2010, 99, (11), 3821-3830.

(6) Chmyrov, A.; Sandén, T.; Widengren, J. Journal of Physical Chemistry B 2010, 114, (34), 11282-11291.

(7) Rigler, R.; Mets, Ü.; Widengren, J.; Kask, P. European Biophysics Journal with Biophysics Letters 1993, 22, (3), 169-175.

(8) Spielmann, T., Blom, H.; Geissbuehler, M.; Lasser, T.; Widengren, J. Journal of Physical Chemistry B 2010, 114, (11), 4035-4046.